

### Scientific Justification

We propose deep and high resolution spectroscopy of the young planetary nebula IC 5117 that is known to exhibit Raman-scattered He II features blueward of hydrogen Balmer lines. The purpose of the current proposal is to secure Raman-scattered He II features at around 4332 Å blueward of H $\gamma$  and at 4850 Å blueward of H $\beta$  in order to develop a spectroscopic tool to probe the distribution of H I in these objects.

Young PNe are important in studying the mass loss process in the late stage of stellar evolution. The hot central star emits strong far-UV radiation that illuminates the surrounding cool region. This constitutes an ideal condition for the operation of Raman scattering by atomic hydrogen. Raman scattering by atomic hydrogen was first identified by Schmid (1989), who proposed that the broad emission features at 6825 Å and 7082 Å are formed from inelastic scattering of far-UV O VI resonance doublet 1032 and 1038. When an O VI line photon is incident on a hydrogen atom in the ground 1s state, the atom may finally de-excite into 2s re-emitting an optical photon redward of H $\alpha$ .

Being a single electron ion with  $Z = 2$ , a He II emission line photon arising from a transition  $2n \rightarrow 2$  has a slightly shorter wavelength than a hydrogen Lyman line photon originating from a level  $np$ . These He II emission line photons can also be Raman-scattered by atomic hydrogen to form broad features blueward of H Balmer emission lines. For example, far-UV He II  $\lambda 1025$  ( $n = 6 \rightarrow n = 2$ ) is Raman-scattered by atomic hydrogen to form a broad feature at around 6545 Å blueward of H $\alpha$ . In a similar way, He II  $\lambda 972$  gives rise to Raman feature at 4850 Å and He II  $\lambda 949$  is Raman-scattered to reappear at 4332 Å.

Thus far, there are only 4 young PNe known to exhibit Raman-scattered He II features and explicitly they are NGC 7027, NGC 6302, NGC 6790 and IC 5117 (Piquignot et al. 1997; Groves et al. 2002; Lee et al. 2006; Kang et al. 2009). The strength and profile of these Raman-scattered He II features depend on various parameters including the H I column density, the covering factor of the neutral region and the relative kinematics of the neutral region and the He II emission region. In this respect, Raman scattering can be an ideal probe of the mass loss process in young PNe. However, the strength of a Raman-scattered He II feature is mainly determined by the product of the H I column density and the covering factor when the scattering optical depth is less than unity, which hinders the determination of the parameters in a separate way. This kind of degeneracy in the parameter space can be lifted by analyzing two or more Raman-scattered He II features at the same time, providing an independent spectroscopic measurement of the mass loss rate in these objects.

However, thus far, Raman spectroscopy of He II has been limited to analyses of the 4850 feature blueward H $\beta$  because Raman-scattered He II at 6545 Å is severely blended with [N II] $\lambda 6548$ , and Raman scattered He II at 4332 Å is very weak, rendering it very difficult to obtain the line profile with sufficient quality. Currently we secured high resolution spectra of IC 5117 using the CFHT in 2014, which show good quality data around the 4850 feature but the data around 4332 Å is of poor quality.

With the huge collecting area of the Gemini-North telescope and the high resolution spectrograph GRACES covering a large range of wavelength, it is highly desirable to observe the young PN IC 5117 to secure the very weak Raman-scattered He II at 4332 Å along with their counterparts at 4850 Å and 6545 Å to determine the H I column density, covering factor and kinematics of the neutral region located in the vicinity of a hot white dwarf. As a byproduct we also expect to find other unexpected Raman-scattered features such as Raman Ne VII at 4881 Å found serendipitously by Lee et al. (2014).

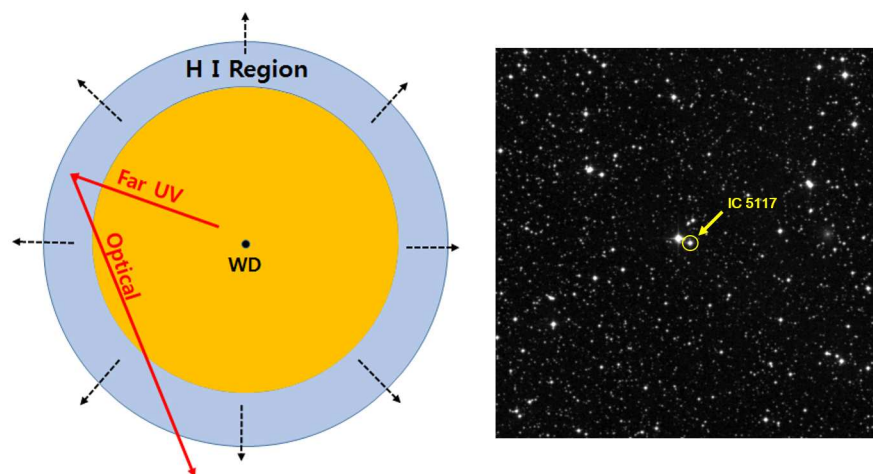


Figure 1: Illustration of Raman scattering geometry relevant to young planetary nebulae (Left Panel) and symbiotic stars (Right Panel). In the case of symbiotic stars, which are binary systems of a hot white dwarf and a mass losing giant, the ionization front approximately takes a form of a hyperboloid toward the white dwarf component. Far UV photons originated in the vicinity of the white dwarf enters the H I region to be subsequently inelastically to reappear near hydrogen Balmer lines.

## References

- Groves et al. 2002 PASA, 19, 425.
- Kang, Lee & Lee 2009 ApJ, 695, 542.
- Lee, Jung, Song & Ahn 2006 ApJ, 636, 1045.
- Lee, Heo & Lee 2014 MNRAS, 441, 1956.
- Pequignot et al. 1997 A&A, 323, 317.
- Schmid 1989 A&A, 211, 31.

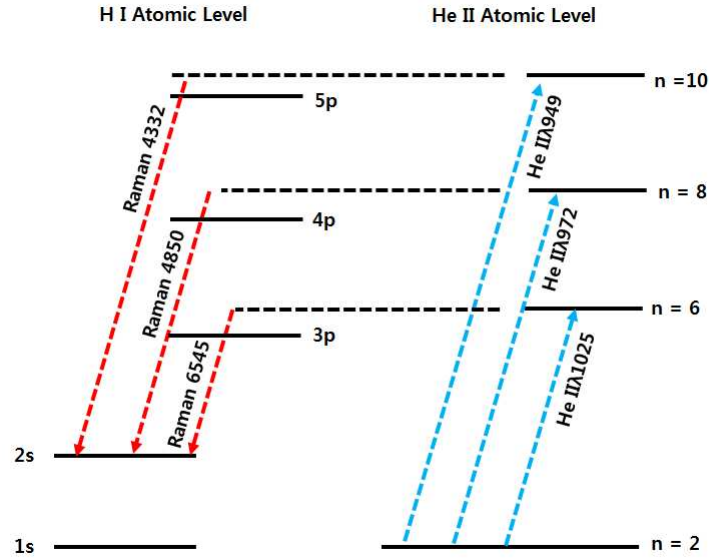


Figure 2: Operation of Raman scattering of far UV He II emission lines by atomic hydrogen. The three He II emission lines He II  $\lambda\lambda$ 1025, 972 and 949 are slightly more energetic than Ly $\beta$ , Ly $\gamma$  and Ly $\delta$ , respectively. If they are incident on a hydrogen atom in the ground state, they can be Raman-scattered to reappear at 6545, 4850 and 4332 Å blueward of H $\alpha$ , H $\beta$ , and H $\gamma$ , respectively.

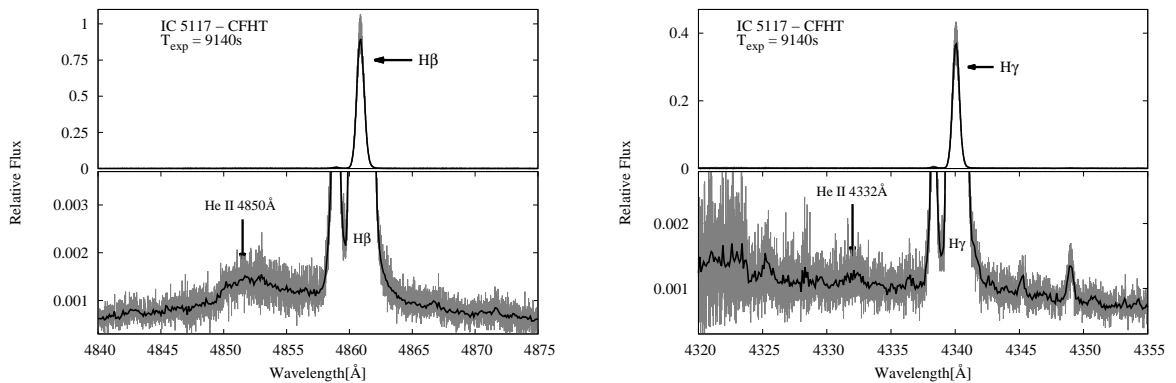


Figure 3: Spectrum of the young planetary nebula IC 5117 around H $\beta$  and H $\gamma$  obtained with the CFHT/ESPADONS in 2014. The bottom panel is an enlarged version of the top panel by a factor  $\sim 100$ . The total integration time is 9140 seconds and the Raman scattered He II at 4332 Å is apparent but of insufficient quality for detailed profile analysis in the left panel.

### Experimental Design

Far-UV He II emission lines arising from  $2n \rightarrow 2$  have slightly smaller wavelengths than those of hydrogen Lyman lines arising from  $np$  states. These emission lines have a large cross section for Rayleigh and Raman scattering due to proximity to resonance. In particular, He II  $\lambda 1025$ , He II  $\lambda 972$ , and He II  $\lambda 949$  are Raman-scattered to appear at 6545, 4850 and 4332 Å, blueward of H $\alpha$ , H $\beta$  and H $\gamma$ , respectively. The typical scattering cross section is  $10^{-21}$  cm<sup>2</sup> for He II  $\lambda 1025$  and decreases by a factor of  $\sim 5$  for He II  $\lambda 972$ . Another factor of  $\sim 5$  smaller scattering cross section for He II  $\lambda 949$  is obtained, so that these Raman features are an ideal tool to probe the H I region with a column density  $\geq 10^{20}$  cm<sup>-2</sup>. Because Raman-scattered He II at 6545 Å is usually severely blended with [N II] $\lambda$  6548, it is quite difficult to perform a careful profile analysis.

The line strengths of Raman features are mainly determined by the product of the H I column density and the covering factor of the neutral hydrogen region. In order to estimate the mass loss rate and study the mass transfer process, it is necessary to lift the degeneracy provided by the two parameters. As Jung & Lee (2004) pointed out, the line center shift of Raman He II is dependent on the H I column density. More specifically, the line center of a Raman He II feature shifts redward as H I column density decreases. This is because red He II line photons have larger cross sections for Raman scattering than blue counterparts. The amount of shift is a complicated function of a wavelength and differs for Raman He II 4850 and Raman He II 4332. This implies that the line centers of the two Raman He II features are not fixed but differ as a function of the H I column density.

Thus far, the shift of line center has been studied in a quantitative way only for Raman He II 4850. Our group is currently studying the line center shift for Raman He II 4332 as a function of the H I column density. The line center shift is also affected by the Doppler effect arising from the motion of the emission region with respect to the neutral region. Therefore, a measurement of the line center shifts of the two Raman He II features at 4850 Å and 4332 Å at the same time will allow us to isolate the column density effect from the Doppler effect.

The case B recombination theory can be used to infer far-UV He II emission flux from optical He II emission lines. By measuring the line strengths of the two Raman-scattered He II features and nearby optical He II emission features, we can estimate the Raman conversion efficiency, which yields a reliable estimate of the covering factor with the known H I column density.

We performed high resolution spectroscopy of the young PN IC 5117 in 2014 with the 3.6 m telescope CFHT to secure Raman scattered He II at 4850 Å with sufficient quality. However, the data are of insufficient quality for detailed profile analysis of the Raman He II 4332 feature, which is essential to break the degeneracy to put strong constraints on the H I content around the hot white dwarf.

We need observational data with long integration time to secure the Raman He II feature at 4332 Å. However, H $\alpha$  is so strong that a single long exposure should be avoided. This means that we have to observe each target a number of times to achieve the goal.

### Technical Description

Using ESPADONS installed on CFHT we obtained high resolution spectra of IC 5117 in 2004, in which the Raman He II feature at 4850 Å was found with barely sufficient signal to noise ratio. The total integration time was 1800 s. However, Raman He II feature at 4332 Å is much weaker by about a factor of 5. A more recent observation in 2014 shows a similar result that at least 10,000 seconds of total integration time for 3.6 m CFHT is barely enough. In this respect, considering the

huge light collecting capability of Gemini-North, we hope to observe this object for total integration time of 7200 seconds.

In order to avoid severe saturation of strong emission lines such as H $\alpha$  and [O III] lines, we plan to obtain 10 spectra with an exposure time of 720 seconds for IC 5117. Furthermore, we want to obtain 2 additional spectra with an exposure time of 36 seconds in order to secure a good H $\alpha$  profile. He II emission lines appear at 4686Å ( $n = 4 \rightarrow n = 3$ ) and 6527Å ( $n = 14 \rightarrow n = 5$ ), which are also important spectral lines to check and verify the Case B recombination nature of the He II emission line region. This implies that our spectroscopy should cover the entire optical wavelength range.

Because information essential for our study to probe the mass loss process includes the line center location, line profile and total flux, high resolution spectroscopy covering the entire optical wavelength range should be performed with optimum resolving power exceeding 40,000. Compared to the spectroscopic resolving power, the other conditions including seeing, cloud cover and sky brightness is of less importance. The only instrument capable of this kind of high resolution spectroscopy with a wide spectral coverage is **GRACES** available on **Gemini-North**. In particular, we choose high resolution mode of "object only" in order to obtain the detailed profiles of He II emission lines and Raman scattered He II features to discover any non-trivial structures.

#### **Band 3 Plan**

This program is not suitable for band 3.

#### **Classical Backup Program**

This is not a classical request.

#### **Justify Target Duplications**

The GSA search revealed no duplicate observations.

#### **Publications**

Jung & Lee 2004 MNRAS, 355, 221.

Kang, Lee & Lee 2009 ApJ, 695, 542.

Lee 2012 ApJ, 750, 127.

Lee, Jung, Song & Ahn 2006 ApJ, 636, 1045.

Lee, Sohn, Kang & Kim 2003 ApJ, 598, 553.

Lee, Heo & Lee 2014 MNRAS, 441, 1956.

#### **Use of Other Facilities or Resources**

#### **Previous Use of Gemini**

#### **ITC Examples**

The spectral type selected is PLANETARY-NEBULA

Reference	Allocation	% Useful	Status of previous data
-----------	------------	----------	-------------------------

The target's magnitude is 16.7000 in the filter G

The sky brightness is 50

The image quality is 70

The cloud cover is 50

The spectral mode is 1 fiber

The air mass is 1.50000

The total exposure time is 7200.00 sec

The chosen read mode is slow

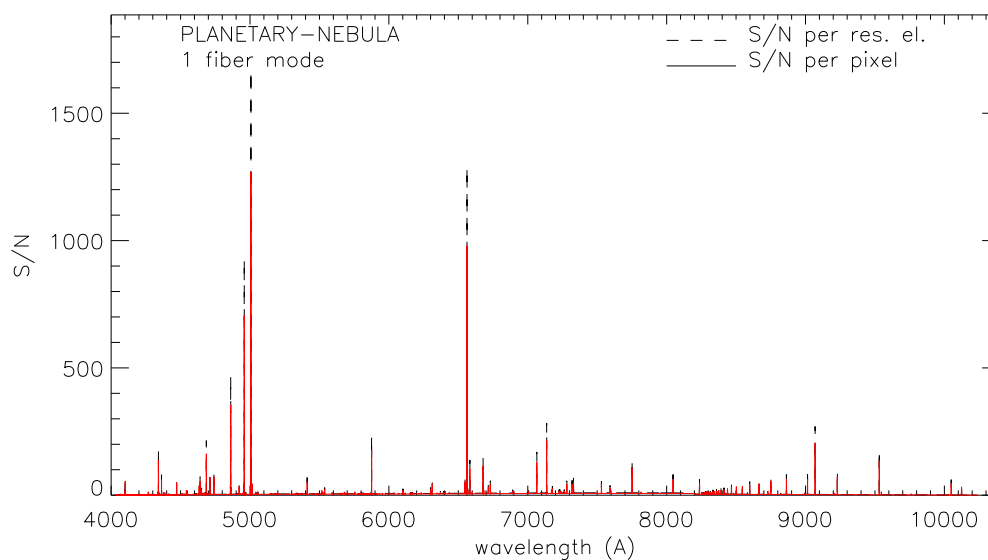


Figure 4: IC5117 (PN, V=16.7), exptime=7200s